POSSIBLE INFLUENCE OF CRITICAL PARAMETERS ON THE VAPOR NUCLEATION IN THE ATMOSPHERE

M.P. Anisimov, A.G. Nasibulin, S.D. Shandakov, and N.I. Gordienok

Institute of Atmospheric Optics,
Siberian Branch of the Russian Academy of Sciences, Tomsk
Received January 26, 1996

In this paper we analyze possible influence of the Laplas pressure on the formation of critical centers. As a result, we arrived a conclusion that the critical line (for the case of binary nucleation) can significantly affect the nucleation. The nucleation rate was measured in the vicinity of critical temperatures of a glycerin-SF_6 binary system. The results obtained show that there is an influence of the critical line on the nucleation rate and parameters of critical centers.

INTRODUCTION

The study of optical properties of gaseous constituents of the atmosphere has a long history, and the methods of such studies are well developed.[1,2] As to the aerosol atmospheric constituent, it is poorly studied. The cause of this is due to poor experimental methods for studying aerosols and, as a consequence, the theoretical models for nucleation are also poor.

Certain progress here can be achieved by means of revision of the axiomatic of the nucleation theory and assumptions used when interpreting experiments on aerosol formation in a supersaturated vapor. For example, the problem on the influence of a carrier gas on the nucleation is still open.[3–8] It is evident that a vapor and a carrier gas comprise a binary system with a limited solubility.[3] Consideration of the nucleation with due regard for this fact may significantly change the interpretation of experiments and, correspondingly, improve the account for nucleation processes in atmospheric models.

The Laplace pressure in the water critical centers is about ten kilobars, whereas for an organic matter it is about one kilobar. That means that conditions for formation of these centers may be close to the critical ones. Up to date this fact was not considered.

The state of the art of both theory and experiment on nucleation in the critical area is considered in detail in Ref. 9. It should only be noted that there are few experiments on nucleation rate in the vicinity of critical states. However estimates of the parameters of critical lines for water in such media as SF_6, CO_2, Ar, He, as well as glycerin and dibutylphthalate in the same gases show that the formation of critical centers under conditions close to critical is a rule rather than an exception.

To find the influence of the critical line on the nucleation, we have chosen the SF_6-glycerin system. This choice is explained by the values of SF_6 critical parameters that are convenient for experiment. In this system the conditions of the nucleation temperature can be easily established both below and above the critical temperatures of the constituents. Below it will be demonstrated that this is of principal importance for experiment.

EXPERIMENT

In this work we used an automated experimental setup whose operation principles are close to that described in Ref. 10. This setup allows us to estimate the nucleation rate against the degree of vapor supersaturation for the substances under study at different pressures of a carrier gas. For a detailed description of the setup see our above paper in this issue (pp. 548–554).

When solving the problem of heat and mass exchange, we used the below values of the parameters.

The diffusion coefficient was calculated for the binary gas system by the empirical expression[11]:

$$D_i = \frac{0.001T^{1.75}\left[(1/M_1) + (1/M_2)\right]^{1/2}}{P\left[(\Sigma v)_1^{1/3} + (\Sigma v)_2^{1/3}\right]^2},$$

where P is the total pressure; M_1 and M_2 are the masses of glycerin and SF_6, respectively; $(\Sigma v)_1$ and $(\Sigma v)_2$ are the corresponding molecular diffusion volumes. The thermal conductivity was calculated by the following equation:

$$\lambda = T_{td}\, C_{SF_6}\, \rho ,$$

derived using the data from Ref. 12, where T_{td} is the thermal diffusivity:

$$T_{td} = \frac{3.20445\ T^2}{P(-0.44\ T + 403.2\ T)},\ \mathrm{W/(m\cdot K)},$$

and the specific heat[13] $C_{SF_6} = 667.6$ J/(kg·K) and slightly depends on temperature and pressure. The pressure of saturated glycerin vapor was calculated as[14] $\log(P) = a - b/T$, where $a = 11.27423$ and $b = 4480.0$. The SF_6 gas constant[12] is $R_{SF_6} = 54.923$ J/(kg·s). The density of a carrier gas was calculated by the equation

0235-6880/96/06 555-06 $02.00

$\rho = P/(R_{SF_6} T)$.

The coefficient of dynamic viscosity is expressed as[15]

$\eta = (1/\pi d^2)\ (kTm/\pi)^{1/2}$,

where d is the molecular diameter.

Figure 1 shows the experimental isothermal dependences of nucleation rates (J) on the degree of glycerin supersaturation (S) in SF_6. Figure 2 demonstrates the isobaric nucleation rate of glycerin in SF_6 at a pressure of 1, 2, and 3 bar and a partial glycerin pressure corresponding to the saturation temperature of 138°C.

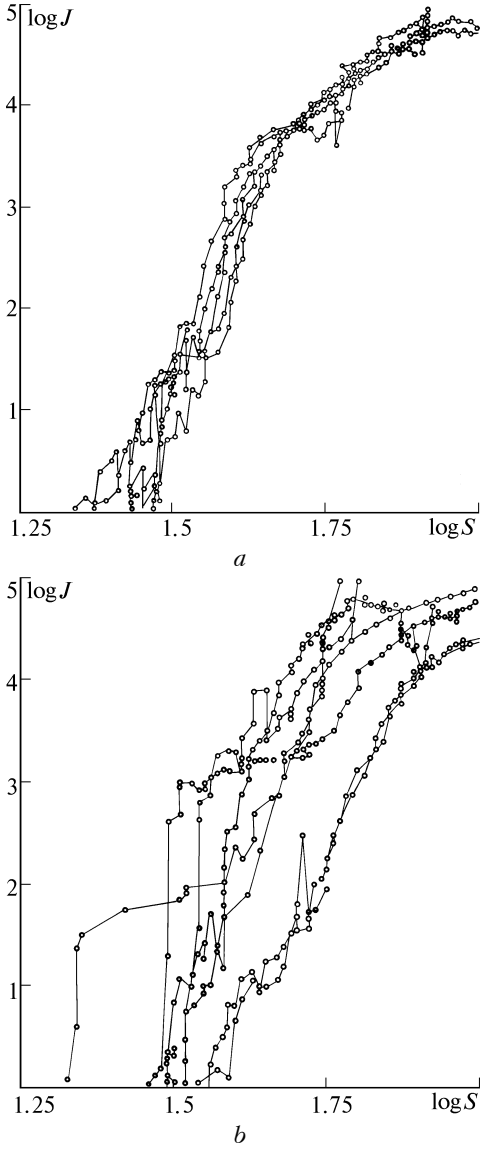

FIG. 1. Experimental dependences of the nucleation rate (J) on the glycerin supersaturation (S) in SF_6 *at the temperature of nucleation (from left to right): a)* 74.5, 62, 64, 67, 69°C; *b)* 62.0, 58.5, 56.0, 53.3, 51.0, 46.0, *and* 43.0°C.

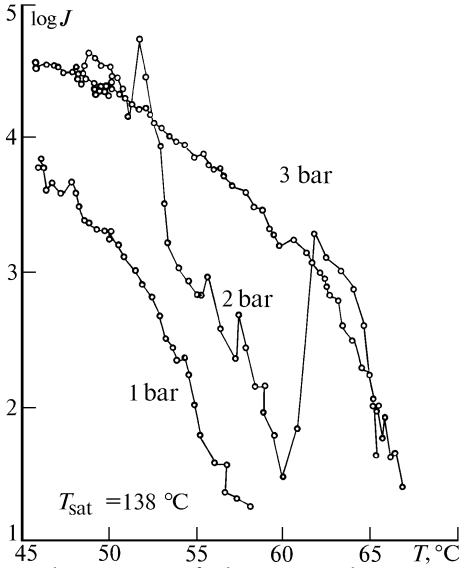

FIG. 2. Isobaric rates of glycerin nucleation in SF_6.

NUCLEATION RATE SURFACES

The idea of demonstrating the statistical and dynamic properties of molecular systems as geometrical images has appeared more than a century ago. The state diagrams are referred to as the geometric thermodynamics dating back to the time of Gibbs.

Let us consider the simplest P–X diagram at a fixed temperature T for a binary solution with unlimited solubility of components. Here P is the pressure of the medium and X is its composition. The state diagram may have a cigar-shaped view. Hereinafter we omit the discussion of effects connected with the period of establishment of a stationary nucleation after the system finds itself in the metastable region.

Let us first find the nucleation rates of vapor of individual constituents A and B (Fig. 3*a*). In the points a and b, corresponding to equilibrium pressure of individual vapors, the nucleation rate, J, is zero. The limited nucleation rates correspond to the boundaries of metastable regions of individual vapors A and B. The maximum values of the nucleation rates (c, d) are connected with the line *ced* of limited rates of the binary nucleation. Let us now consider the isothermal nucleation of binary vapor having a composition X_0. The nucleation starts at the point f. The condensed phase has a composition X_1. Every point of the line *nfm* can be related to a point of nucleation beginning on the curve *ngm*. It follows therefrom that the surface of nucleation rates of a binary vapor originates at the line *ngm* and finishes at the line of limiting nucleation rates of a binary vapor (*ced*). In the labile region the vapor and the condensed phase have the same composition. Intermediate pressures between P_r and P_e yield the line *re*.

Figure 3*b* shows the surface of nucleation rates for the case when the temperature is above the critical temperature of one of the constituents (A). In this case

the diagram is drop-shaped. The limiting value of the nucleation rate of the constituent B (the point c) is connected, with the line of limiting values of the binary nucleation, to the point of intersection of $P–X$ diagram at a fixed temperature and the critical line. The nucleation rate at the critical point is zero in accordance with the theorem on the nucleation rate at a critical point.[16] The further analysis completely coincides with the description of data presented in Fig. 3*a*.

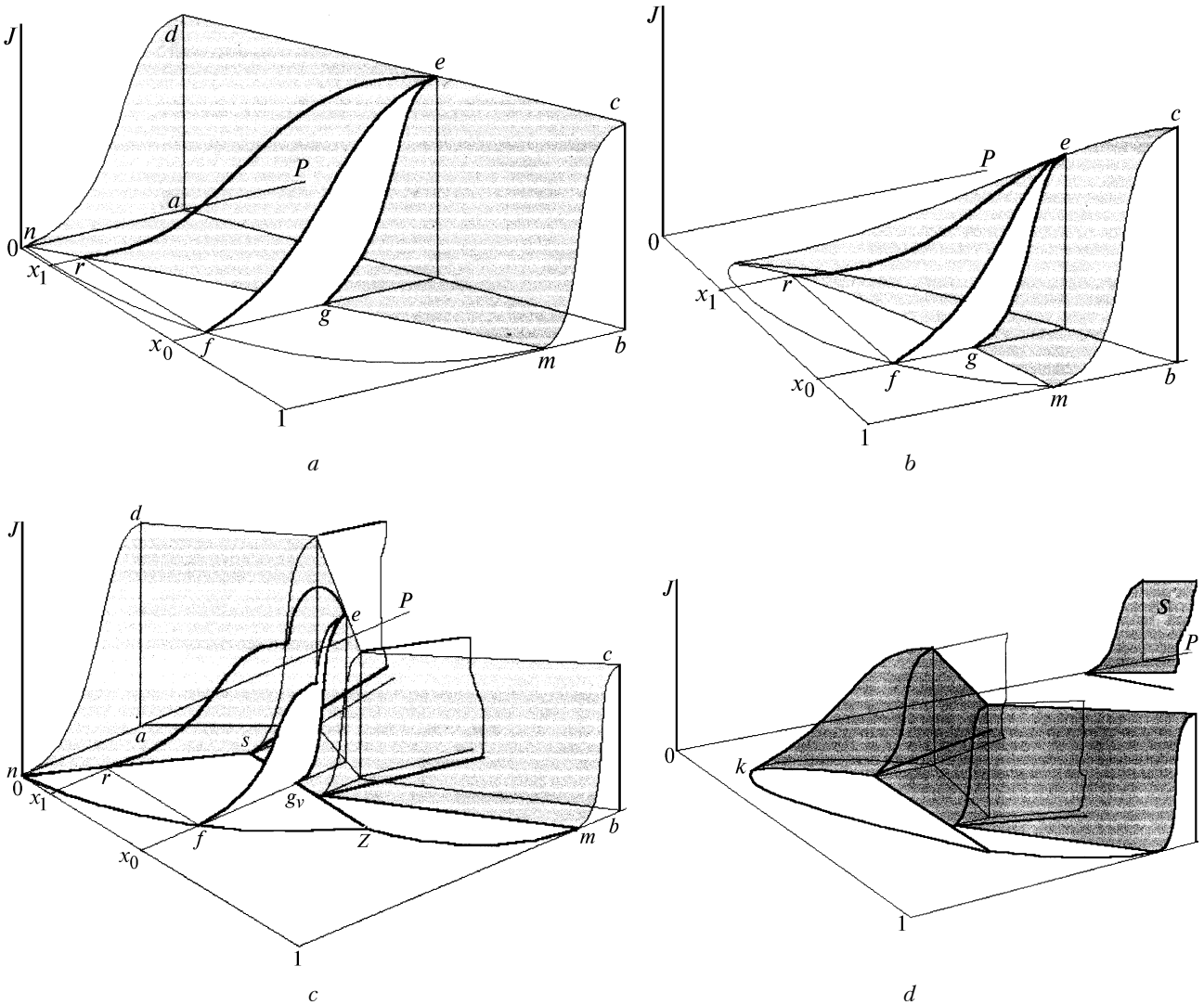

FIG. 3. Nucleation rate surfaces for: a binary system of soluble constituents (a and b), a binary system with limited solubility of constituents (c and d), at the nucleation temperature below the critical temperatures of constituents (a and c) and above the critical temperature of a constituent A (b and d).

Now let us construct the surface of nucleation rates for the system with a limited solubility of constituents. This system has a diagram with a paritectic point (Fig. 3*c*). In the region of solution existence, the same reasoning are true as for Fig. 3*a*. Let us consider the nucleation of a vapor with composition X_0 in the region of heterogenic solutions. Isothermal compression of this vapor results in formation of a condensed phase of the composition X_1 at the point f. When the composition of the condensed phase coincides with the composition X_s at the point s, the curve of nucleation rates comes onto the surface corresponding to the formation of particles with compositions X_s and X_v. That corresponds to the nucleation through two channels with different energy barriers as it was shown in Ref. 17.

It is evident from Fig. 3*c* that relative productivity of the channels is determined by the lever principle for nucleation rates. The composition of the condensed phase coincides with that of the initial vapor on the spinodal at the point e. The resultant curve er has an unusual, from the viewpoint of the nucleation theory, inflection at the composition X_s. For the nucleation temperature above the critical temperature of one constituent of a solution with limited solubility, the surface of nucleation rates takes the shape shown in

Fig. 3*d*. Of a certain interest are the compositions to the left from the critical point *k*. Here a vapor being compressed does not meet the vapor-liquid equilibrium lines and thus comes to the region of supercritical fluid state. Its further compression results in the intersection of the line of equilibrium between the homogeneous and heterogeneous fluid states and the line of transition into the crystal state. The surface of rates of crystal formation is marked with a letter *S* in Fig. 3*d*.

In the first three cases, the curves *er* should be a result of experiments with a vapor of the X_0 composition. However, in the experiments we have the lines *ef* being the projections of *er* onto the plane *efg* (see, for example, Refs. 18–19), i.e. determined is the surface area *nfmcd*. These are obviously two forms of presentation of the nucleation rates. One assumes that the composition of critical centers is known, whereas another one, which is commonly accepted, does not. The nucleation rate surfaces, corresponding to different representations, coincide above the spinodal line. At low rates of vapor nucleation, the difference between surfaces can reach several orders of magnitude. The last case (Fig. 3*d*) takes place at nucleation in a gas medium or under atmospheric conditions. For the quantitative analysis, it is necessary to know the state diagrams for systems interesting for practical applications. In the atmosphere, these are the nitrogen-water medium with addition of sulfur and nitrogen acids, ammonia, and other components.

THEORETICAL ESTIMATES OF THE CRITICAL CONDITIONS

The true critical temperature of a mixture usually is not a linear function of mole components of critical temperatures of pure constituents. Lee[11] proposed that if the composition can be presented by the function

$$\Phi_j = \frac{y_j\, V_{cj}}{\sum\limits_i y_j\, V_{ci}} ,$$

then the critical temperature of the mixture can be found as

$$T_{ct} = \sum\limits_j \Phi_j\, T_{cj} ,$$

where y_i is the mole fraction of the *j*th constituent, V_{cj} is its critical volume, T_{cj} is its critical temperature, and T_{ct} is the true critical temperature of the mixture. The mean calculational error for this method is below 4 K. For multicomponent hydrocarbon mixtures the error is about 11 K.

To calculate the critical volumes, we have used the analytical technique described in Ref. 11. The critical volume of a mixture was calculated by the expression

$$V = \sum\limits_j \theta_j\, V_{cj} + \sum\limits_i \sum\limits_j \theta_i\, \theta_j\, \nu_{ij} ,$$

where V_{cj} is the critical volume of the *j*th constituent, ν_{ij} is the interaction parameter; $\nu_{ii} = 0$, and ν_{ij} $(i \neq j)$ can be calculated as

$$\varphi_v = A + B\delta_v + C\delta_v^2 + D_v^3 + E\delta_v^4 ,$$

$$\varphi_v = 2\nu_{ij} \;/\; (V_{ci} + V_{cj}) ;$$

$$\delta_v = \left| \frac{V_{ci}^{2/3}\; V_{cj}^{2/3}}{V_{ci}^{2/3} + V_{cj}^{2/3}} \right| ,$$

and the surface fraction θ_j can be determined as

$$\theta_j = (y_j\, V_{cj}^{2/3}) \;/\; (\sum\limits_i y_i\, V_{ci}^{2/3}) .$$

The values of the coefficients *A*, *B*, *C*, *D*, and *E* for some types of pairs of constituents at $0 \le \delta \le 0.5$ can be found in Ref. 11.

This method has been checked with 23 binary hydrocarbon mixtures and 8 binary mixtures of hydrocarbon with nonhydrocarbon.[11] The error was 10.5%.

The method for prediction of the mixture critical pressures was proposed in Ref. 11, where the critical pressure P_{ct} is related to the critical volume V_{ct} and the critical temperature T_{ct} by means of the modified Redlih–Kwong equation of a state:

$$P_{ct} = \frac{R\, T_{ct}}{V_{ct} - b_m} - \frac{a_m}{T_{ct}^{1/2}\; V_{ct}\; (V_{ct} + b_m)} ,$$

where T_{ct} and V_{ct} can be calculated as shown above. The coefficients for P_{ct} estimation are found as

$$b_m = \sum\limits_j y_j\, b_j = \sum\limits_j (y_j\, \Omega_j\, T_{cj}) \;/\; P_{cj} ;$$

$$a_m = \sum\limits_i \sum\limits_j y_i\, y_j\, a_{ij}$$

with allowance for the fact that

$$\Omega_j = 0.0867 - 0.0125\omega_j + 0.011\omega_j^2 ,$$

where ω_j is the Pitzer acentricity factor;

$$a_{ij} = \frac{(\Omega_i + \Omega_j)\; R\; T_{cij}^{1/2}\; (V_{ci} + V_{cj})}{4(0.291 - 0.04(\omega_i + \omega_j))} ,$$

$$a_{ii} = (\Omega_{ai}\, R^2\, T_{ci}^{2,5}) \;/\; P_{ci} ;$$

$$T_{cij} = (1 - k_{ij})\; (T_{ci}\, T_{cj})^{1/2} ;$$

$$\Omega_j = \left(\frac{R\, T_{cj}}{V_{cj}\, b_j}\, P_{cj}\right) \frac{P_{cj}\; V_{cj}\; (V_{cj} + b_j)}{(R\, T_{cj})^2} .$$

The calculated and experimental values of P_{ct} differ by 2 atm. Figure 4 shows the theoretical estimates for critical temperatures and pressures for the binary systems: water, glycerin, and dibutylphthalate in a medium of He, Ar, CO_2, and SF_6. It is seen from the figure that critical pressures of binary systems do not exceed a half of a kilobar, whereas critical temperatures are no more than several hundreds degrees.

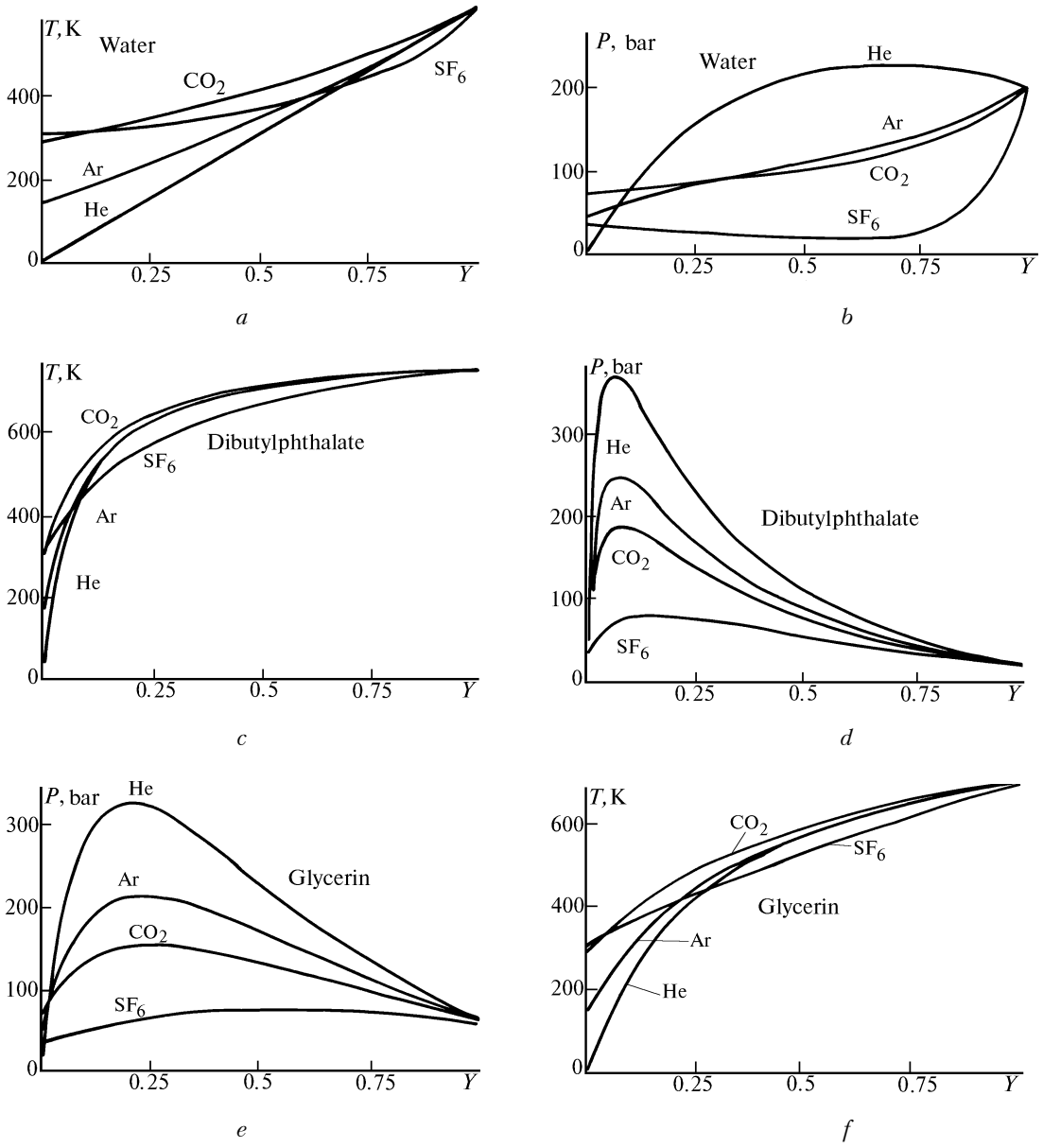

FIG. 4. Theoretical estimates of the critical temperature and pressure for binary systems: water, glycerin, dibutylphthalate in He, Ar, CO_2, *and* SF_6.

For nucleation in the SF_6 medium, the change of the nucleation temperature from below-critical for both constituents to supercritical for one of the constituents (SF_6) can occur. This allows us to successively come from the rate surface shown in Fig. 3*c* to that shown in Fig. 3*d*.

DISCUSSION

As follows from Ref. 20, the dependence of vapor supersaturation on the nucleation temperature at a fixed rate contains an information about the surface energy of critical centers of a new phase. Nonmonotonic behavior of the function $S(T)$ should be indicative of a nonmonotonic behavior of the surface energy of these centers.

Figure 5 shows the $\log S$ against the glycerin nucleation temperature at four fixed values of the nucleation rate ($\log J$ = 1, 2, 3, and 4). It is evident that, at all the nucleation rates, $\log S$ are nonmonotonic functions of the nucleation temperature. Figure 5 demonstrates a monotonic drop of $\log S(T)$ with temperature with the further break. Further growth of the nucleation temperature results in an irregular behavior of $\log S(T)$. Such a behavior of $\log S(T)$ was earlier observed for a dibutylphthalate nucleation. Change in the character of $\log S(T)$ dependence at some fixed nucleation rates is indicative of the anomalous temperature dependence of the surface energy of the critical clusters. Coincidence of the temperature corresponding to the inflection region with the conditions for critical line is a demonstration of its

influence on the nucleation process and can be considered as a tentative, but quite convincing verification of the influence of near-critical conditions on the nucleation process.

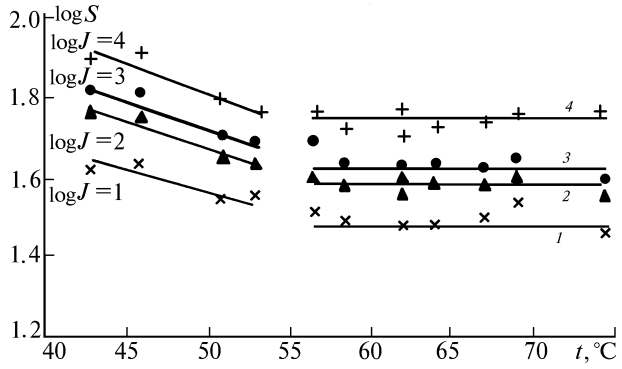

FIG. 5. Supersaturation (S) against the glycerin nucleation temperature (T).

The isobaric nucleation rate being measured shows the dependence of the function log$J$ on the nucleation temperature T which looks like thermograms of melting of a binary solution. At a nucleating medium pressure of 2 bar, sharp oscillations of a nucleation rate are observed. In Ref. 21 it is shown that the derivative d log J/dT is governed by the phase enthalpy. It follows therefrom that in the vicinity of critical conditions the nucleation depends on some other relaxation phenomena not jet well understood. Study of their nature is one of the interesting problems.

CONCLUSIONS

The Laplace pressure in critical centers, calculated neglecting the influence of the critical line, proves to be near-critical or even supercritical for a majority of cases important for atmospheric nucleation. Therefrom we can draw a conclusion, nontrivial for the theory of nucleation and, particularly, atmospheric nucleation, that formation of critical centers of a new phase and, correspondingly, the rate of nucleation of supersaturated vapor are mainly determined by the conditions of the near-critical line or the equilibrium line of fluid equilibriums of a nucleating system. It is important that air (or other carrier gas) is a participant of this process, that influences the parameters of the critical line (or critical surface). A detailed analysis of this fact may significantly change our understanding of the atmospheric nucleation.

ACKNOWLEDGMENT

This work was supported in part by the Russian Foundation for Fundamental Research, Grant No. 94–03–09947. One author would like to acknowledge the Russian Academy of Sciences for the State grant.

REFERENCES

1. V.E. Zuev and G.M. Krekov, *Optical Models of the Atmosphere* (Gidrometeoizdat, Leningrad, 1986), 256 pp.
2. M.V. Panchenko and S.A. Terpugova, in: *Proc. of Ninth Annual Conference on Aerosols, Their Generation, Behaviour, and Applications*, Norvich, Great Britain (1995), pp. 163–175.
3. M.P. Anisimov and S.N. Vershinin, J. Aerosol Sci. **21**, Suppl. 1, 11–18 (1990).
4. I.J. Ford, in: *Nucleation and Atmospheric Aerosols,* ed. by M. Fukuta and P.E. Wagner (Deepak, Hampton VA, 1992), pp. 39–42.
5. J.L. Katz, J.A. Fisk, and V. Chakarov, *ibid.*, pp. 11–40.
6. P.E. Wagner, R. Strey, and Y. Viisanen, *ibid.*, pp. 27–30.
7. G. Wilemski, B.E. Wyslouzil, M. Gauthier, and M.B. Frish, *ibid.*, pp. 23–26.
8. *Proc. of International Workshop on Nucleation Experiments. State of the Art and Future Developments,* Prague, Czech Republic (1995), p. 25.
9. R. McGraw, J. Chem. Phys. **91**, No. 9, 5655–5664 (1989).
10. M.P. Anisimov, in: *Aerosols, Science, Industry, Health, and Environment. Proc. 3rd Int. Aerosol Conf.,* Kyoto (Pergamon Press, Oxford etc., 1990), Vol. 1, pp. 146–150.
11. R. Reed, J. Prousnitz, and T. Sherwood, *Properties of Gases and Liquids* [Russian translation] (Khimiya, Leningrad, 1982), 592 pp.
12. N.V. Vargaftik, *Handbook on Thermophysical Properties of Gases and Liquids* (Fizmatgiz, Moscow, 1963), 708 pp.
13. V.A. Rabinovich and Z.Ya. Khavin, *Concise Chemical Handbook* (Khimiya, Leningrad, 1991), 432 pp.
14. A.G. Amelin, *Theoretical Principles of Fog Formation at Vapor Condensation* (Khimiya, Moscow, 1972), 304 pp.
15. E.A. Melvin–Hews, *Physical Chemistry* [Russian translation] (Foreign Literature Press, Moscow, 1962), Vol. 1, 519 pp.
16. M.P. Anisimov, in: *Aerosols, Their Generation, Behaviour, and Applications* (Univ. of East England, Norwich, 1995), pp. 201–215.
17. A.K. Ray, M. Chalam, and L.K. Peters, J. Chem. Phys. **85**, 2161–2168 (1986).
18. M.P. Anisimov, et al., Kolloidn. Zh. **49**, No. 5, 842–846 (1987).
19. R. Strey and P.E. Wagner, J. Aerosol Sci. **19**, 813–816 (1988).
20. M.P. Anisimov and A.V. Taylakov, J. Aerosol Sci. **20**, No. 8, 1063–1066 (1989).
21. M.P. Anisimov and A.G. Cherevko, J. Aerosol Sci. **16**, No. 2, 97–107 (1985).